

PHYSICAL CHEMISTRY OF NANOCLUSTERS,
SUPRAMOLECULAR STRUCTURES, AND NANOMATERIALS

STUDY OF FORMATION FEATURES
AND ELECTROCHEMICAL PROPERTIES OF GE-CO NANOCOMPOSITE
ON COPPER SUBSTRATE

I. M. Gavrilin^a, *, I. S. Marinkin^b, Y. O. Kudryashova^a, E. V. Kovtushenko^a,
T. L. Kulova^a, **, and A. M. Skundin^a

^aFrumkin Institute of Physical Chemistry and Electrochemistry, Russian Academy of Sciences, Moscow, 119071 Russia

^bNational Research University "MIET", Moscow, Zelenograd, 124498 Russia

*e-mail: gavrilin.ilya@gmail.ru

**e-mail: tkulova@mail.ru

Received April 22, 2024

Revised April 22, 2024

Accepted May 07, 2024

Abstract. In this work, we have demonstrated for the first time the possibility of electrochemical formation of Ge-Co nanostructures on a copper substrate, which are globules whose size reaches 1 μm , consisting of smaller particles whose size does not exceed 10 nm. Such nanostructures demonstrate a sufficiently high reversible capacity of about 850 mAh/g and good stability under long-term cycling.

Keywords: germanium, nanostructures, electrochemical deposition, lithium-ion battery

DOI: 10.31857/S00444537250110e2

INTRODUCTION

Group 4 elements of the Periodic Table, such as silicon (Si) and germanium (Ge), are candidates to replace graphite (372 mAh/g) in lithium-ion batteries due to their high theoretical specific capacity (4200 mAh/g for Si and 1600 mAh/g for Ge) [1–3]. In turn, Ge has higher electrical conductivity (5000 times higher than Si) and lithium ion diffusion rate (400 times higher than Si) [4, 5]. Unfortunately, the introduction of lithium into Ge, actually, as in Si, is accompanied by a noticeable volume expansion (up to 300%) and a respective increase in internal stresses. Such volumetric expansion leads to rapid degradation of the electrode and, consequently, to a decrease in the characteristics of the battery as a whole. Moreover, repeated periodic volume changes lead to respective periodic failures of the solid electrolyte interphase (SEI). Two strategies can be used to solve this problem, viz. switching to nanomaterials (including nanopowders, nanowires, thin films) or using multicomponent systems (alloys, composites, etc.) [6–11].

Effective nanomaterials are filamentary Ge nanostructures obtained by electrochemical deposition from the GeO_2 aqueous solution using indium particles as crystallization centers [12]. Being an intermediate product in the production of elemental germanium, GeO_2 is much cheaper than germanium. Also, such

structures are obtained directly on the current sink substrate so that electrodes do not contain any binders as well as conductive additives. In addition, using mixed electrolyte solutions, one can obtain multicomponent systems [13, 14]. Certain attention should be paid to the recent work [15], in which germanium-cobalt-indium (Ge–Co–In) nanostructures were formed for the first time by cathodic deposition from aqueous complex solutions of Ge (IV) and Co (II) using indium particles. In this case, the nanostructures are spherical globules with diameters between 200 and 800 nm composed of smaller particles with sizes between 5 and 10 nm. There are filamentary Ge nanostructures in the space between the globules. The electrode based on Ge–Co–In nanostructures in the process of galvanostatic cycling demonstrates a sufficiently high specific lithium injection capacity of 1350 mAh/g at C/8 and room temperature, as well as a high Coulomb efficiency of 76% at the first cycle without special additives used in the electrolyte, such as vinylene carbonate or fluoroethylene carbonate. Moreover, Ge–Co–In nanostructures also show high performance at negative temperatures down to -35°C . In [15], nanostructures were obtained on a titanium substrate with a deposited layer of chromium; however, when applying such structures as an anode material, it is more appropriate to use copper foil, which is used in the negative electrodes of all commercial lithium-ion

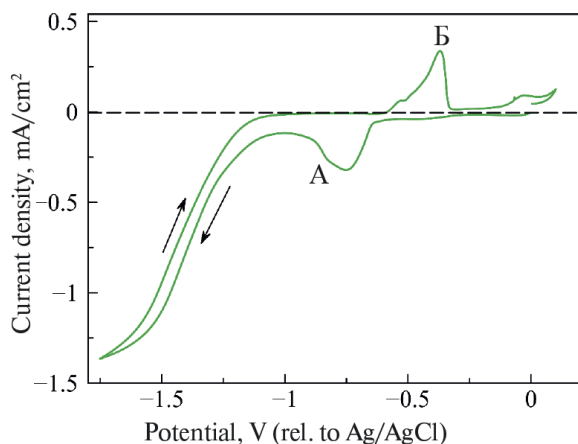


Fig. 1. Cyclic voltammograms recorded in the solution $0.01\text{ M InCl}_3 + 0.5\text{ M C}_6\text{H}_8\text{O}_7$ using a copper substrate. The scan frequency of the potential is 5 mV/s .

batteries. In turn, the substrate can significantly influence the formation process of nanostructures. Therefore, the purpose of this work was to study the peculiarities of electrochemical deposition of nanostructures from aqueous complex solutions of Ge (IV) and Co (II) on a copper substrate, as well as to test such structures as a negative electrode material in lithium-ion batteries.

EXPERIMENTAL PART

Electrochemical deposition of indium was carried out in a three-electrode cell. A copper foil ($9\text{ }\mu\text{m}$ thick, 99.999% pure) cut into $3 \times 3\text{ cm}$ pieces was used as a working electrode. A chemically resistant varnish was applied on the back side of the substrate and around the working area. The working area was 6 cm^2 . A $3 \times 3\text{ cm}$ platinum grid was used as the counter electrode and a silver chloride electrode ($\text{Ag}/\text{AgCl}/3\text{ M KCl}$) was used as the reference electrode. The solution for deposition of indium inoculums consisted of 0.015 M citric acid and 0.01 M indium chloride (InCl_3). Deposition of the inoculums was carried out in the galvanostatic mode at -1 mA/cm^2 for various time periods. The deposition was carried out at the solution temperature 20°C .

To prepare the electrolyte solution for obtaining Ge–Co–In nanostructures, solutions A and B were mixed in a $2 : 3$ ratio (in what follows, we refer to such a solution as GeCo solution). The composition of solution A is 0.01 M CoSO_4 and $0.1\text{ M CH}_3\text{COONa}$. The composition of solution B is 0.1 M GeO_2 , $0.1\text{ M C}_4\text{H}_6\text{O}_4$ and $0.5\text{ M K}_2\text{SO}_4$. The precipitation was carried out at a constant potential of -1.1 V for 10 min .

The pH values of the solutions were measured using a HANNA HI 2002-02 pH meter. In all experiments,

the current density or potential was set using an Autolab PGSTAT302N galvanostat-potentiostat. Currents were normalized to the geometric surface area of the electrode. The temperature of all solutions was controlled using a Termex VT-01 thermostat. Immediately after deposition, the nanostructures were washed with deionized water and dried in the argon flow (grade 6.0). The nanostructures were weighed on Metter Toledo XP 205 analytical scales with an accuracy of $10\text{ }\mu\text{g}$.

The morphology of the obtained samples was studied by scanning electron microscopy on a Zeiss Supra-40 microscope (Inlens SE detector was used, with the accelerating voltage 10 kV and the aperture $30\text{ }\mu\text{m}$).

Electrochemical testing of electrodes with the obtained structures (working electrode) was carried out in three-electrode sealed cells of a plane-parallel design with a lithium auxiliary electrode and a lithium reference electrode. The counter electrode and reference electrode were made of metallic lithium rolled on a nickel mesh substrate. The electrodes were separated by a separator made of nonwoven polypropylene (UFIM, Russia). The electrolyte used was 1 M LiClO_4 in propylene carbonate-dimethoxyethane ($7 : 3$) mixture with $2\text{ vol.}\%$ of vinylene carbonate added. All reagents were Battery grade and purchased from Aldrich. The water content of the electrolyte did not exceed 20 ppm . The electrochemical cells were assembled in a glove box with dry argon atmosphere (Spektroskopicheskie sistemy, Russia). The water and oxygen content in the box did not exceed 5 ppm . Galvanostatic testing of electrochemical cells was performed using a P-208X potentiostat-galvanostat (Elins, Russia).

DISCUSSION OF RESULTS

Studying Peculiarities of Electrochemical Deposition of Indium on Copper Substrate from Aqueous Solution Based on InCl₃

In order to form both filamentary Ge nanostructures and Ge–Co–In nanostructures, one needs to perform an array of In particles that are the crystallization centers of Ge [14]. Therefore, it is important to study the electrochemical formation of indium on the copper substrate.

Figure 1 shows cyclic voltammogram (CVA) obtained in a solution of $0.01\text{ M InCl}_3 + 0.5\text{ M C}_6\text{H}_8\text{O}_7$ (the solution pH is 2.3) using copper foil as the working electrode. The graphs were plotted from an open circuit potential (OCP) value to negative potentials (-1.75 V as compared to Ag/AgCl) and then continued in the opposite direction to a more positive potential

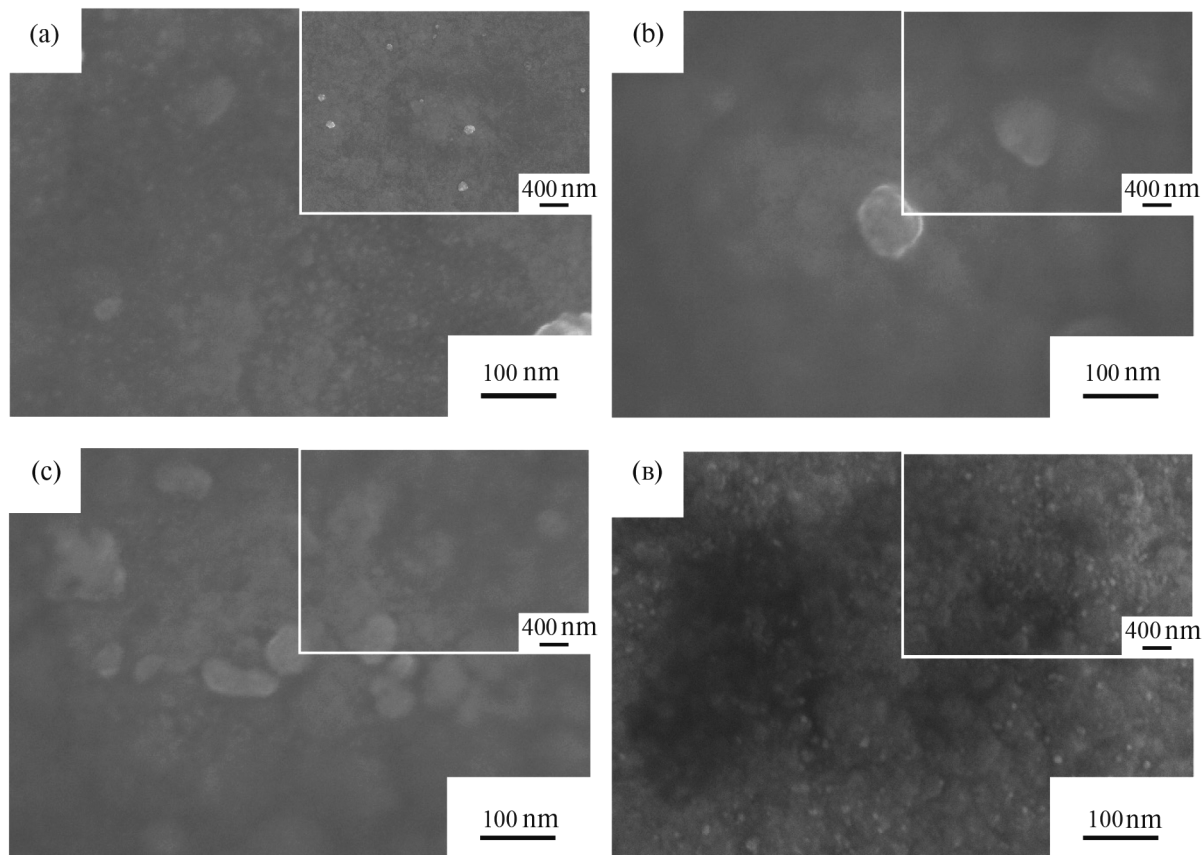


Fig. 2. SEM images of the surface of the samples obtained for different deposition times, viz. (a) 5 s, (b) 15 s, (c) 30 s, and (d) 60 s. The insets show SEM images at lower magnification.

to -0.01 V to complete the test at the initial OCP potential value. The scan frequency of the potential was 5 mV/s.

On the obtained CVA for the copper substrate in the cathode part, the first significant current increase starts at a potential of about -0.6 V and reaches its maximum at a potential of -0.75 V with respect to the silver chloride reference electrode (Fig. 1, peak A). It is also worth noting the pronounced shoulder around -0.85 V. Thus, the observed peak is a superposition of peaks, which may indicate the multistage electrochemical process of indium deposition under these conditions. In the anodic region of the CVA, a peak with the current maximum around -0.37 V was observed (Fig. 1, peak B), associated with the oxidation of indium to indium-containing ions with almost finite zero current, indicating complete dissolution of the indium coating.

Further, we performed experiments in the galvanostatic mode at different current densities, viz. 0.5 , 1 , and 2 mA/cm^2 for 60 s. However, uniform coating was observed only for the current density of

1 mA/cm^2 . In particular, the film was not formed visually for the current density 0.5 mA/cm^2 , and an intensive gas release was observed in the case of 2 mA/cm^2 , which resulted in a coating disruption. Therefore, we carried out further studies at the current density 1 mA/cm^2 . To study the sequence of formation of indium layer on the copper substrate at the initial stages, we prepared samples for different deposition times, viz. 5 , 15 , 30 , and 60 s, and obtained the respective scanning electron microscope images (SEM images) of their surface morphology (Fig. 2).

As we can see from the obtained SEM results, there are no pronounced spherical particles on the surface of the copper substrate, as it was observed in the case of using the electrolyte solution of the same composition and Ti-Cr substrate [15]. Nevertheless, in some cases, one can observe islet formations as early as after 5 s of the process, the size of which can reach 100 nm. Also, at a larger image scale, many nanoparticles with a size not exceeding 10 nm can be seen, which one can observe on all samples. Analysis of publications [16–19] showed that electrochemical deposition of

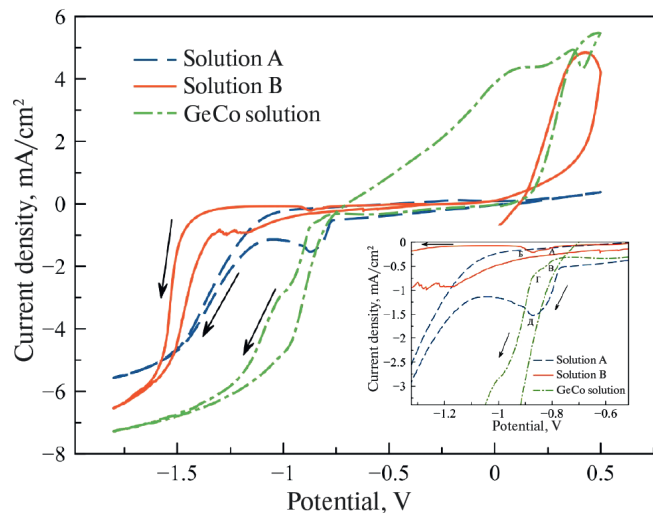


Fig. 3. Cyclic voltammograms recorded in various solutions using a copper substrate with a deposited indium layer. The types of solutions are indicated in the figure.

indium on the copper substrate occurs in two stages, unlike other substrate materials (chromium, platinum, or glassy carbon). At the first stage, the CuIn alloy is formed as a result of mutual diffusion of atoms. After that, the growth of In islets is observed. However, the mechanism of electrochemical deposition of indium on copper substrates requires a more detailed study, which is beyond the scope of this work.

Studying the Peculiarities of Electrochemical Deposition of Ge–Co on Copper Substrate with Indium Inoculums

To determine the values of the deposition potentials of Ge–Co structures, CVA were obtained in the GeCo solution using indium-doped copper foil as a working electrode. Based on the results obtained, the indium deposition time to obtain Ge–Co structures was 60 s. Figure 3 shows the obtained CVAs at the scan frequency 5 mV/s. For comparison, CVA were also obtained in separate solutions for the deposition of cobalt (solution A) and germanium (solution B).

As we can see from the CVA obtained in solution B (solution without cobalt ions), a significant increase in the cathodic current is observed only after reaching a potential of about -1.3 V. This significant increase in the cathodic current is mostly due to the electrochemical reduction of water (the solution pH is 6.3). When the axes are scaled (the inset), a broad peak is recorded in the potential range from -0.7 V to -0.95 V, with the peak having two maximums (maximums A and B, the inset in Fig. 3), indicating several electrochemical reactions (or a multistage process). In this potential

range, germanium deposition appears to occur, with the small cathodic current indicating low reaction efficiency. One knows that the electrochemical deposition of Ge from aqueous solutions is limited to obtaining a film with a thickness of no more than a few nanometers [20]. When cobalt ions are added to the solution (the GeCo solution, pH 6.7), there is a significant increase in the cathodic current in the potential range involved (Fig. CVA in the GeCo solution). It is also worth noting that, approximately in the same potential range, a peak is observed in CVA (peak D, the inset in Fig. 3) obtained in the pure cobalt solution (solution A, pH 7.7), which corresponds to the reduction of cobalt-containing ions, and the cathodic current is also smaller than in the case of the mixed solution. Thus, the addition of cobalt ions to the solution leads to an increase in the efficiency of the electrochemical process.

Based on the results of CVA analysis, we used the potential -1.1 V for further studies in the potentiostatic mode. Figure 4 shows SEM images of the morphology of the obtained sample in the GeCo solution for the potential -1.1 V.

As we can see, globules are formed on the surface, their size reaching $1\text{ }\mu\text{m}$ in some cases. At higher magnification, we can see that the globule is a cluster of small particles, their size not exceeding 10 nm. Note the absence of filamentary Ge nanostructures observed when we used a titanium substrate with a deposited chromium layer in our previous work [14]. This is due to the absence of pronounced In particles on the copper substrate, which are the centers of crystallization of Ge, as noted earlier. According to the data of energy dispersive X-ray spectroscopy, the obtained structure contains the elements Ge, Co, and O, the concentration of which is 44, 23, 33 at.%, respectively.

Thus, the addition of cobalt ions to the solution initiates the process of co-deposition of germanium and cobalt. A similar process was observed when copper and silver ions were added to the germanium solution [21, 22].

Studying Reversible Lithium Embedding in Ge–Co Nanocomposite on Copper Substrate

Figure 5 shows the charge-discharge curves and the change of the discharge capacity during cycling of the obtained Ge–Co sample.

In general, the shape of the charge-discharge curve is typical for germanium-based nanostructures obtained by cathodic deposition [12, 14]. It is worth noting that metallic cobalt does not embed lithium [23]. On the cathodic (charge) curve of the first cycle presented in Fig. 5a, one can highlight a small plateau in the potential region of 1.37 – 1.24 V (vs. Li/Li^+), which is

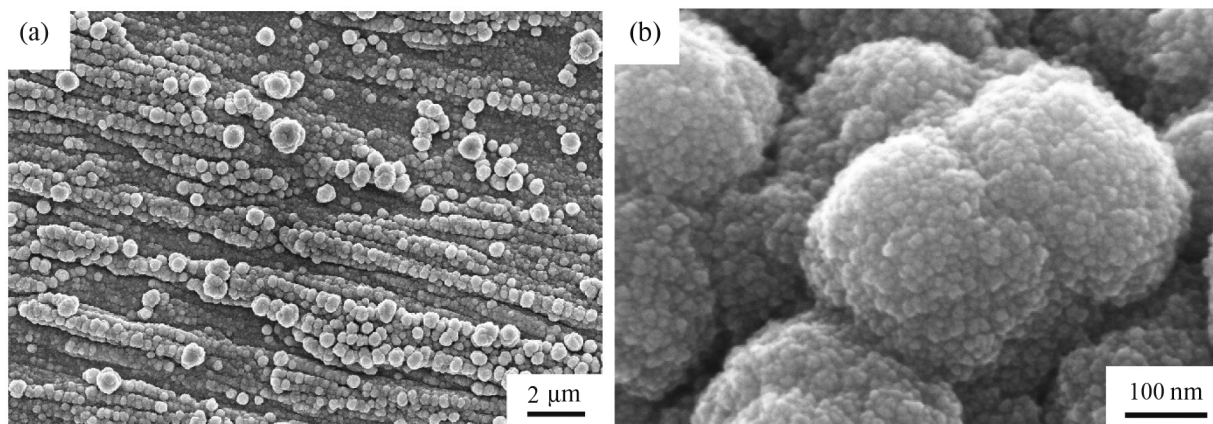


Fig. 4. SEM images of the surface of the sample obtained after electrochemical deposition from the GeCo solution at different magnifications — (a) 15 000 x and (b) 400 000 x.

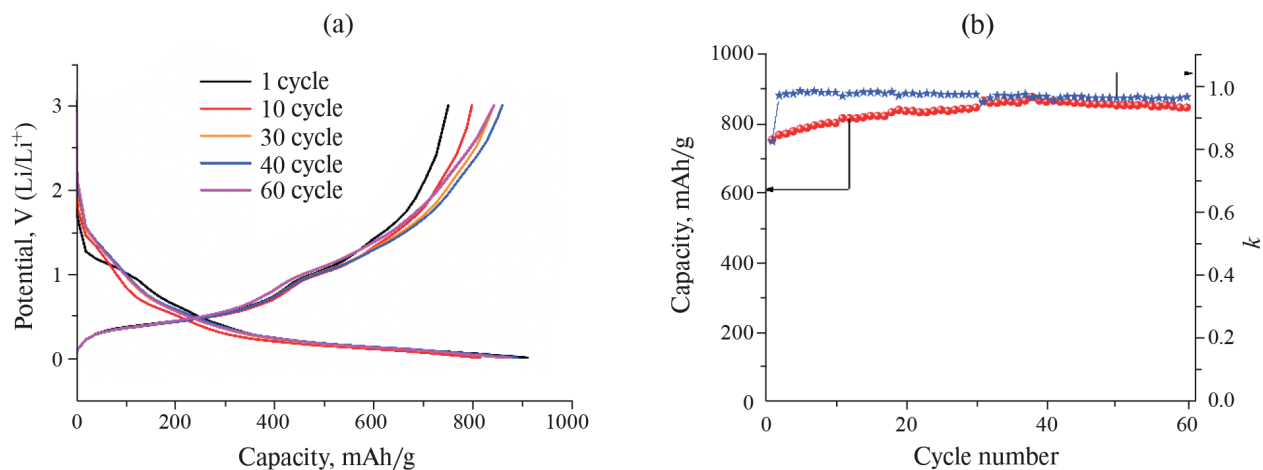


Fig. 5. Charge-discharge curves (a), change of the discharge capacity and Coulomb efficiency (b) during lithium embedding/extraction in/from the Ge-Co nanostructure. The charge/discharge current is 250 mA/g.

due to the solid electrolyte interphase (SEI) formed on the surface of Ge-Co nanostructures. At the first cycle, the charging and discharging capacities were 915 and 753 mAh/g, respectively. During further cycling, an increase in the discharge capacity was observed up to cycle 32, which amounted to about 850 mAh/g, after which the value was constant. Note also the sufficiently high Coulomb efficiency at the first cycle, which amounted to about 82%.

CONCLUSIONS

In this work, we demonstrated for the first time the possibility of electrochemical formation of Ge–Co nanostructures on a copper substrate, which are globules with their size up to 1 μ m, consisting of smaller particles, their size not exceeding 10 nm. Such nanostructures exhibit a rather high reversible

capacity with respect to lithium incorporation of about 850 mAh/g and good cycling stability. The above allows us to conclude that the demonstrated possibility of electrochemical formation of Ge–Co nanostructures on a copper substrate will accelerate the introduction of such structures into commercial lithium-ion batteries.

FUNDING

The research was supported by the Russian Science Foundation (grant no. 20-79-10312, <https://rscf.ru/project/20-79-10312/>)

CONFLICT OF INTEREST

The authors of this work declare that they have no conflicts of interest.

REFERENCES

1. Park M., Kim K., Kim J. et al. // *Adv. Mater.* 2010. Vol. 22. P. 415.
2. Harper G., Sommerville R., Kendrick E. et al. // *Nature*. 2019. Vol. 575. P. 75.
3. Choi S., Kwon T.W., Coskun A. et al. // *Science*. 2017. Vol. 357. P. 279.
4. Graetz J., Ahn C.C., Yazami R. et al. // *J. Electrochem. Soc.* 2004. Vol. 151. P. A698.
5. Chou C.-Y., Hwang G.S. // *J. Power Sources*. 2014. Vol. 263. P. 252.
6. Hao J., Wang Y., Guo Q. // *Part. Part. Syst. Charact.* 2019. Vol. 36. P. 1900248.
7. Wu S., Han C., Iocozzia J. et al. // *Angew. Chem. Int. Ed.* 2016. Vol. 55. P. 7898.
8. Liu Y., Zhang S., Zhu T. // *ChemElectroChem*. 2014. Vol. 1. P. 706.
9. Kim D.-H., Park C.M. // *Mater. Today Energy*. 2020. Vol. 18. P. 100530.
10. Jing Y.-Q., Qu J., Jia X.-Q. et al. // *Chem. Eng. J.* 2021. Vol. 408. P. 127266.
11. Zhao W., Chen J., Lei Y. et al. // *J. Alloys Compd.* 2020. Vol. 815. P. 152281.
12. Gavrilin I.M., Kudryashova Yu.O., Kuz'mina A.A. et al. // *J. Electroanal. Chem.* 2021. Vol. 888. P. 115209.
13. Kulova T.L., Skundin A.M., Gavrilin I.M. et al. // *Batteries*. 2022. Vol. 8. P. 98.
14. Gavrilov S.A., Gavrilin I.M., Martynova I.K. et al. // *Ibid.* 2023. Vol. 9. P. 445.
15. Gavrilin I., Martynova I., Petukhov I. et al. // *J. Solid State Electrochem.* 2023. Vol. 28. P. 1521.
16. Lee S. M., Ikeda S., Otsuka Y. et al. // *Electrochim. Acta*. 2012. Vol. 79. P. 189.
17. Chung Y., Lee C.-W. // *J. Electrochem. Sci. Technol.* 2013. Vol. 4. P. 93.
18. Huang Q., Reuter K., Amhed S. et al. // *J. Electrochem. Soc.* 2011. Vol. 158. P. D57.
19. Valderrama R.C., Miranda-Hernández M., Sebastian P.J. et al. // *Electrochim. Acta*. 2008. Vol. 53. P. 3714.
20. Liang X., Kim Y.-G., Gebergziabiher D. K. et al. // *Langmuir*. 2010. Vol. 26. P. 2877.
21. Bahmani E., Zakeri A., Aghdam A. S. R. // *J. Mater. Sci.* 2021. Vol. 56. P. 6427.
22. Zhao F., Xu Y., Mibus M. et al. // *J. Electrochem. Soc.* 2017. Vol. 164. P. D354.
23. Nzereogu P.U., Omah A.D., Ezema F.I. et al. // *Appl. Surf. Sci. Adv.* 2022. Vol. 9. P. 100233.